J. Fluid Mech. (1989), *vol.* 198, *pp.* 543–555
Printed in Great Britain

Modulated stagnation-point flow and steady streaming

By GREGORY J. MERCHANT AND STEPHEN H. DAVIS
Department of Engineering Sciences and Applied Mathematics, Northwestern University, Evanston, IL 60208, USA

(Received 29 December 1987 and in revised form 1 June 1988)

Plane stagnation-point flow is modulated in the free stream so that the velocity components are proportional to $K_H + K\cos\omega t$. Similarity solutions of the Navier–Stokes equations are examined using high-frequency asymptotics for K and K_H of unit order. Special attention is focused on the steady streaming generated in this flow with strongly non-parallel streamlines. For small modulation amplitude $K \leqslant K_H$, unique self-similar streaming flows exist. For large modulation amplitude $K > K_H$, if $(K/\omega)(K/K_H) \geqslant 1.661$ no self-similar streaming is possible, while if $\frac{4}{3} \leqslant (K/\omega)(K/K_H) \leqslant 1.661$, then multiple steady solutions occur.

1. Introduction

A solid body oscillates with angular frequency ω and amplitude A in an otherwise motionless fluid of kinematic viscosity ν. For small values of A, there is an $O(A)$ Stokes layer on the body of thickness $\delta = (\nu/\omega)^{\frac{1}{2}}$. At order (A^2) a steady-streaming field is set up through the rectification of the periodic forcing by the advective nonlinearities. Schlichting (1932) first discovered such flows when considering small two-dimensional oscillations of a cylinder along its diameter and attributed the steady streaming to the action of Reynolds stresses in the Stokes layer. Rosenblat (1959) showed in the analogous case of a torsionally oscillation disk that the steady streaming occurs on a scale δ_s near the body where $\delta_s = \delta/A$; thus $\delta_s \gg \delta$. Stuart (1966) showed that the steady streaming could be desribed by a steady-streaming Reynolds number R_s which governs the thickness of the drift layer; if $R_s \gg 1$, there is a secondary boundary layer while if $R_s < 1$, the drift has a creeping-flow character.

This double-layer structure for small A occurs not only in the case of oscillating bodies and torsionally oscillating disks, but is typical of viscous fluids flowing with zero mean. It also occurs with pulsatile flows in tapered tubes (Hall 1974; Grotberg 1984), and in wave fields in viscous flows (Longuet-Higgins 1953). Many of the above issues have been reviewed by Riley (1965, 1975). For bounded flows, such as those in fluid-filled channels with pulsating walls (Secomb 1978) or between torsionally oscillating disks (Rosenblat 1960) no second boundary layer is formed.

When a mean flow is present, small-amplitude modulation can lead to similar behaviours. Lighthill (1954) examined a modulated external flow about a cylindrical body and obtained the Stokes-layer correction to the external flow. Ishigaki (1970) examined the similar case of stagnation-point flow with special attention paid to the skin friction on the plate. Neither Lighthill nor Ishigaki calculated effects of steady streaming. Pedley (1972) analysed the modulated laminar boundary layer on a semi-infinite flat plate for a range of Falkner–Skan problems including stagnation-point

flow. Matunobu (1977) studied pulsatile Hiemenz flow for the cases of small frequency and amplitude by examining the linearized vorticity equation.

Consider now stagnation-point flow, modulated in the free stream, so that the velocity components are proportional to $K_H + K\cos\omega t$. Such a flow simulates the effects of impinging sound waves on the boundary layer of a blunt-nosed body (Morkovin 1978) and so is used to study boundary-layer receptivity. It may simulate the locally hyperbolic streamlines present in a cellular, pulsating flow on a plate, a useful idealization when contemplating the effects of time-periodic convection on a directionally solidifying crystal.

Grosch & Salwen (1982) studied modulated stagnation-point flow by examining the Navier–Stokes equations, seeking unsteady similarity solutions and analysing steady streaming for high and low frequencies and *small amplitudes*. Pedley (1972) analysed the boundary-layer equations, studied high and low frequencies for unit-order modulation amplitudes but avoided reverse outer flows and concentrated on skin-friction effects.

The present work extends that of Pedley (1972) and Grosch & Salwen (1982) by analysing the Navier–Stokes equations and examining *high frequencies* and *unit-order amplitudes* so as to study *steady streaming* in the presence of *reverse outer flow* driven by *large temporal modulations*. In this way one can obtain new insights into the structure of the steady streaming. In agreement with Grosch & Salwen (1982) we find that the steady streaming can be calculated without the analysis of the double boundary layers and we find that the streaming is confined to the steady Hiemenz layer of thickness $(\nu/K_H)^{\frac{1}{2}}$ even for *large* modulation amplitudes. When the modulation is small $K < K_H$, the steady streaming is unique. When the steady, Hiemenz flow is small $K > K_H$, and $(K/K_H)(K/\omega) \geqslant 1.661$, there exists no self-similar streaming, and if $K > K_H$ and $\frac{4}{3} \leqslant (K/K_H)(K/\omega) \leqslant 1.661$, then these steady-streaming flows are non-unique. This steady streaming has an outer structure identical to that of a boundary layer over an upstream-moving semi-infinite plate.

2. Formulation

An incompressible Newtonian fluid of a kinematic viscosity ν flows against a plate at $y = 0$. The coordinates (x, y) lie, respectively, along and normal to the plate; the corresponding equations can be written in terms of the stream function ψ and ω_3, the z-component of vorticity, as follows:

$$\omega_{3t} + \psi_y \omega_{3x} - \psi_x \omega_{3y} = \nu(\omega_{3xx} + \omega_{3yy}) \tag{2.1a}$$

and

$$-\omega_3 = \psi_{xx} + \psi_{yy}, \tag{2.1b}$$

where subscripts denote partial differentiation. Here,

$$(u, v) = (\psi_y, -\psi_x). \tag{2.2}$$

Far from the plate, $y \to \infty$, the velocity field is taken to be that of plane stagnation-point flow of an inviscid fluid upon which a modulation is superimposed. At infinity

$$u = x(K_H + K\cos\omega t), \quad v = -y(K_H + K\cos\omega t), \tag{2.3a, b}$$

where K and K_H denote the magnitudes of the oscillatory and steady fields, respectively, and ω is the angular frequency of the oscillation.

At the plate the conditions of no penetration and no slip apply.

We seek similarity solutions for (2.1) of the form

$$u = xf_y(y,t), \quad v = -f(y,t), \tag{2.4a, b}$$

which reduces (2.1) to the form

$$-f_{yyt} - f_y f_{yy} + f f_{yyy} + \nu f_{yyyy} = 0. \tag{2.5}$$

Upon integration once with respect to y and the use of the far-field condition

$$f \to y(K_H + K\cos\omega t) \quad \text{as} \quad y \to \infty, \tag{2.6}$$

(2.5) gives

$$-f_{yt} - f_y^2 + f f_{yy} + \nu f_{yyy} = K\omega \sin\omega t - (K_H + K\cos\omega t)^2, \tag{2.7a}$$

with the boundary conditions

$$f = f_y = 0 \quad \text{at} \quad y = 0, \tag{2.7b}$$

$$f_y \to K_H + K\cos\omega t \quad \text{as} \quad y \to \infty. \tag{2.7c}$$

In scaling system (2.7) we use the larger of the magnitudes of K_H and K. On the one hand, if $K_H > K$, we have *modulated Hiemenz flow* and we introduce the non-dimensional variables as follows:

$$\tau = \omega t, \quad \Omega = \frac{\omega}{K_H}, \quad \delta = \frac{K}{K_H}, \tag{2.8a}$$

$$\eta = (K_H/\nu)^{\frac{1}{2}} y, \quad f = (K_H \nu)^{\frac{1}{2}} F. \tag{2.8b}$$

If we substitute forms (2.8) into system (2.7), we obtain

$$-\Omega F_{\eta\tau} - F_\eta^2 + F F_{\eta\eta} + F_{\eta\eta\eta} = \Omega\delta \sin\tau - (1 + \delta\cos\tau)^2, \tag{2.9a}$$

$$F = F_\eta = 0 \quad \text{at} \quad \eta = 0, \tag{2.9b}$$

$$F_\eta \to 1 + \delta\cos\tau \quad \text{as} \quad \eta \to \infty, \tag{2.9c}$$

where $0 \leqslant \delta \leqslant 1$.

On the other hand if $K > K_H$, we have *quasi-pulsatile flow* and we replace K_H by K in the scales (2.8) and introduce the new variables $\hat{\eta}$ and $\hat{F}$. The system (2.7) becomes

$$-\hat{\Omega}\hat{F}_{\hat{\eta}\tau} - \hat{F}_{\hat{\eta}}^2 + \hat{F}\hat{F}_{\hat{\eta}\hat{\eta}} + \hat{F}_{\hat{\eta}\hat{\eta}\hat{\eta}} = \hat{\Omega}\sin\tau - (\Delta + \cos\tau)^2, \tag{2.10a}$$

$$\hat{F} = \hat{F}_{\hat{\eta}} = 0 \quad \text{at} \quad \hat{\eta} = 0, \tag{2.10b}$$

$$\hat{F}_{\hat{\eta}} \to \Delta + \cos\tau \quad \text{as} \quad \hat{\eta} \to \infty, \tag{2.10c}$$

with

$$\Delta = K_H/K \tag{2.11}$$

where $0 \leqslant \Delta < 1$.

The nonlinear partial differential systems (2.9) and (2.10) are now examined for large ω via the parameters Ω and $\hat{\Omega}$ with δ or Δ being unit order.

3. Asymptotic expansion for large frequency

We aim to find solutions periodic in τ. First, consider system (2.9) for modulated Hiemenz flow, $K_H \geqslant K$, and define a small parameter ϵ by

$$\Omega = \frac{\omega}{K_H} = \frac{1}{\epsilon^2}. \tag{3.1}$$

The governing equation is then of a singular type as $\epsilon \to 0$ and can be solved by means of matched asymptotic expansions. The inner variables are chosen to be

$$\xi = \eta/\epsilon, \quad \psi(\xi, \tau) = F(\eta, \tau). \tag{3.2a, b}$$

Note that, via ξ, y is now scaled on the Stokes boundary-layer thickness

$$\epsilon(\nu/K_H)^{\frac{1}{2}} = (\nu/\omega)^{\frac{1}{2}},$$

while the outer variable η, is y scaled on the Hiemenz boundary-layer thickness $(\nu/K_H)^{\frac{1}{2}}$. This part of the analysis closely parallels those of Pedley (1972) and Grosch & Salwen (1982); we summarize the results for completeness.

3.1. *The outer expansion*

In terms of the outer variables (2.9) becomes

$$-F_{\eta\tau} + \epsilon^2[-F_\eta^2 + FF_{\eta\eta} + F_{\eta\eta\eta}] = \delta \sin\tau - \epsilon^2[1 + \tfrac{1}{2}\delta^2 + 2\delta\cos\tau + \tfrac{1}{2}\delta^2\cos 2\tau], \tag{3.3a}$$

$$F_\eta \to 1 + \delta\cos\tau \quad \text{as} \quad \eta \to \infty. \tag{3.3b}$$

We seek a solution of the form

$$F(\eta, \tau) = F_0(\eta, \tau) + \epsilon F_1(\eta, \tau) + \tfrac{1}{2}\epsilon^2 F_2(\eta, \tau) + \tfrac{1}{6}\epsilon^3 F_3(\eta, \tau) + \ldots. \tag{3.4}$$

The leading-order solution is

$$F_0(\eta, \tau) = \delta\eta\cos\tau + f_0(\eta) + g_0(\tau), \tag{3.5a}$$

where the arbitrary functions $f_0(\eta)$ and $g_0(\tau)$ are determined from matching to the inner solution and from secularity conditions. Arbitrary functions of this type appear in each subsequent term of the outer expansion. The other terms in the outer expansion are

$$F_1(\eta, \tau) = f_1(\eta) + g_1(\tau), \tag{3.5b}$$

$$F_2(\eta, \tau) = 2[2\eta - 3f_0 + \eta f_0']\,\delta\sin\tau + f_2(\eta) + g_2(\tau), \tag{3.5c}$$

and

$$F_3(\eta, \tau) = 6[\eta f_1' - 3f_1]\,\delta\sin\tau - 6\delta f_0'\sin(\tau - \tfrac{1}{4}\pi) + f_3(\eta) + g_3(\tau). \tag{3.5d}$$

Restrictions are placed on $f_i(\eta)$, $i = 0, 1, 2, 3$, so that the solutions are periodic in τ; these are given below.

The functions $f_0(\eta)$ and $f_1(\eta)$ satisfy

$$f_0''' - f_0'^2 + f_0 f_0'' + 1 = 0, \tag{3.6a}$$

and

$$f_1''' + f_0 f_1'' - 2f_0' f_1' + f_0'' f_1 = 0. \tag{3.6b}$$

It is shown later that $f_1(\eta) \equiv 0$. By using this the equations for $f_2(\eta)$ and $f_3(\eta)$ become

$$f_i''' + f_0 f_i'' - 2f_0' f_i' + f_i f_0'' = 0, \quad i = 2, 3. \tag{3.6c}$$

3.2. *The inner expansion and matching*

If we rewrite system (2.9) in terms of the inner variables ξ and ψ given by (3.2a, b), we obtain

$$-\psi_{\xi\tau}+\psi_{\xi\xi\xi}+\epsilon[-\psi_\xi^2+\psi\psi_{\xi\xi}] = \epsilon\delta\sin\tau-\epsilon^3[1+\tfrac{1}{2}\delta^2+2\delta\cos\tau+\tfrac{1}{2}\delta^2\cos 2\tau] \quad (3.7a)$$

$$\psi = \psi_\xi = 0 \quad \text{at} \quad \xi = 0. \quad (3.7b)$$

Again we seek a solution of the form

$$\psi(\xi,\tau) = \psi_0(\xi,\tau)+\epsilon\psi_1(\xi,\tau)+\tfrac{1}{2}\epsilon^2\psi_2(\xi,\tau)+\tfrac{1}{6}\epsilon^3\psi_3(\xi,\tau)+\ldots. \quad (3.8)$$

The functions $\psi_i(\xi,\tau), i = 0,1,2,3$ (after matching with the outer solution) are given by

$$\psi_0(\xi,\tau) = 0, \quad (3.9a)$$

$$\psi_1(\xi,\tau) = \delta[\xi\cos\tau-\cos(\tau-\tfrac{1}{4}\pi)+\mathrm{e}^{-\xi/\sqrt{2}}\cos(\tau-\xi/\sqrt{2}-\tfrac{1}{4}\pi)] \quad (3.9b)$$

$$\psi_2(\xi,\tau) = 2c\xi^2, \quad (3.9c)$$

and

$$\begin{aligned}\psi_3(\xi,\tau) = {} & -\xi^3+\tfrac{3}{2}\delta^2\left[\frac{13}{\sqrt{2}}-3\xi-3\sqrt{2}\,\mathrm{e}^{-\xi/\sqrt{2}}\cos(\xi/\sqrt{2})+\sqrt{2}\,\mathrm{e}^{-\xi/\sqrt{2}}\sin(\xi/\sqrt{2})\right.\\ & \left.-\frac{1}{\sqrt{2}}\mathrm{e}^{-\sqrt{2}\xi}-2\xi\,\mathrm{e}^{-\xi/\sqrt{2}}\sin(\xi/\sqrt{2})-6\,\mathrm{e}^{-\xi/\sqrt{2}}\cos(\xi/\sqrt{2}-\tfrac{1}{4}\pi)\right]\\ & +12\delta[\xi\sin\tau+\cos(\tau+\tfrac{1}{4}\pi)-\mathrm{e}^{-\xi/\sqrt{2}}\cos(\tau-\xi/\sqrt{2}+\tfrac{1}{4}\pi)]\\ & -\tfrac{3}{2}\delta^2[\sqrt{2}\cos(2\tau+\tfrac{1}{4}\pi)-\sqrt{2}\,\mathrm{e}^{-\xi}\cos(\xi-2\tau+\tfrac{1}{4}\pi)-2\xi\,\mathrm{e}^{-\xi/\sqrt{2}}\sin(\xi/\sqrt{2}-2\tau)],\end{aligned} \quad (3.9d)$$

where c is a constant. Imbedded within the solution $\psi_1(\xi,\tau)$ is the Stokes shear wave (with a phase shift of $\frac{1}{4}\pi$), which enforces the no-slip condition at the surface of the plate consistent with the oscillatory flow near the surface.

The following results were obtained from the matching process. The functions $g_i(\tau), i = 0,1,2,3$, appearing in (3.5) are given by

$$g_0(\tau) \equiv 0, \quad g_1(\tau) = -\delta\cos(\tau-\tfrac{1}{4}\pi), \quad g_2(\tau) \equiv 0, \quad (3.10a, b, c)$$

and

$$g_3(\tau) = 12\delta\cos(\tau+\tfrac{1}{4}\pi)-\frac{3\sqrt{2}}{2}\delta^2\cos(2\tau+\tfrac{1}{4}\pi); \quad (3.10d)$$

with $f_0(\eta)$ given by

$$f_0(\eta) = F_{\mathrm{H}}(\eta), \quad (3.11a)$$

where $F_{\mathrm{H}}(\eta)$ is the solution to the Hiemenz equations for steady stagnation-point flow. The solution is unique and is well-tabulated in numerical form (cf. Rosenhead 1963, p. 232). It has the small-η expansion

$$F_{\mathrm{H}}(\eta) \sim c\eta^2-\tfrac{1}{6}\eta^3+\frac{c^2}{30}\eta^5+\ldots \quad \text{as} \quad \eta\to 0, \quad (3.11b)$$

where $c \approx 1.232588$ and is the constant appearing in (3.9c). We find that

$$f_1(\eta) \equiv 0, \quad f_2(\eta) = -\frac{3\delta^2}{4c}F'_{\mathrm{H}}(\eta), \quad (3.11c, d)$$

and $f_3(\eta)$ satisfies the system

$$f_3''' + f_0 f_3'' - 2f_0' f_3' + f_0'' f_3 = 0, \tag{3.11e}$$

$$f_3(0) = \frac{39\sqrt{2}}{4}\delta^2, \quad f_3'(0) = 0, \quad f_3'(\infty) = 0. \tag{3.11f}$$

The solution $f_3(\eta)$ must be obtained numerically.

The solutions obtained for $f_1(\eta)$, $f_2(\eta)$ and $f_3(\eta)$ are assumed to be unique, in that no eigenfunctions exist that solve equations of the form (3.6*c*) with homogeneous boundary conditions. In his analysis Pedley (1972) concludes for stagnation-point flow that no eigenfunctions exist and so the solutions can be fully determined. Our selected numerical work performed on (3.11*e*, *f*) supports this view.

The composite expansion for $F(\eta, \tau)$ is then given by

$$\begin{aligned} F(\eta,\tau) = {} & F_{\mathrm{H}}(\eta) + \delta\eta\cos\tau \\ & + \epsilon[\delta\,\mathrm{e}^{-\eta/\epsilon\sqrt{2}}\cos(\tau-\eta/\epsilon\sqrt{2}-\tfrac{1}{4}\pi) - \delta\cos(\tau-\tfrac{1}{4}\pi)] \\ & + \tfrac{1}{2}\epsilon^2\Big[2\delta(2\eta+\eta F_{\mathrm{H}}'-3F_{\mathrm{H}})\sin\tau - \frac{3\delta^2}{4c}F_{\mathrm{H}}' \\ & - \delta^2\eta\,\mathrm{e}^{-\eta/\epsilon\sqrt{2}}\sin(\eta/\epsilon\sqrt{2}) + \delta^2\eta\,\mathrm{e}^{-\eta/\epsilon\sqrt{2}}\sin(\eta/\epsilon\sqrt{2}-2\tau)\Big] \\ & + \tfrac{1}{6}\epsilon^3[-9\sqrt{2}\,\delta^2\,\mathrm{e}^{-\eta/\epsilon\sqrt{2}}\cos(\eta/\epsilon\sqrt{2}) - 3\sqrt{2}\,\delta^2\,\mathrm{e}^{-\eta/\epsilon\sqrt{2}}\sin(\eta/\epsilon\sqrt{2}) \\ & - \tfrac{3}{4}\sqrt{2}\,\delta^2\,\mathrm{e}^{-\sqrt{2}\eta/\epsilon} - 12\delta\,\mathrm{e}^{-\eta/\epsilon\sqrt{2}}\cos(\tau-\eta/\epsilon\sqrt{2}+\tfrac{1}{4}\pi) \\ & - 6\delta F_{\mathrm{H}}'\sin(\tau-\tfrac{1}{4}\pi) + \tfrac{3}{2}\sqrt{2}\,\delta^2\,\mathrm{e}^{-\eta/\epsilon}\cos(\eta/\epsilon-2\tau-\tfrac{1}{4}\pi) \\ & + 12\delta\cos(\tau+\tfrac{1}{4}\pi) - \tfrac{3}{2}\sqrt{2}\,\delta^2\cos(2\tau+\tfrac{1}{4}\pi) + f_3(\eta)] + \ldots. \end{aligned} \tag{3.12}$$

A notable feature of oscillatory-flow problems is the occurrence of *steady streaming* which originates in the Stokes layer of thickness $(\nu/\omega)^{\frac{1}{2}}$ owing to the action of Reynolds stresses (Schlichting 1932) and persists beyond it. In the present problem the steady streaming is confined to the Hiemenz boundary layer of thickness $(\nu/K_{\mathrm{H}})^{\frac{1}{2}}$, which is of the order ϵ^{-1} thicker than the Stokes layer. The steady streaming of (3.12) with the $F_{\mathrm{H}}(\eta)$ term subtracted out is shown in figure 1. It can be seen that near the plate there is a drift away from the stagnation point and return flow above the plate.

For oscillatory flow in the absence of a mean the steady-streaming boundary layer has been noted to be considerably thicker than $(\nu/K_{\mathrm{H}})^{\frac{1}{2}}$, namely of the order ϵ^{-2} times the Stokes layer (cf. Rosenblat 1959; Stuart 1966; Riley 1975). In order to gain an understanding of this difference, $\Delta = K_{\mathrm{H}}/K$ will be considered to be small and the quasi-pulsatile form of the system will be considered. For the asymptotic analysis K will be considered fixed and K_{H} will vary; thus all variables will be scaled on K.

3.3. *Small mean flow*

Consider system (2.10) which contains the parameter $\Delta = K_{\mathrm{H}}/K$. Again, we seek solutions for large $\hat{\Omega}$, where the small parameter ϵ is now scaled on K such that

$$\hat{\Omega} = \frac{\omega}{K} = \frac{1}{\hat{\epsilon}^2}.$$

The mean flow approaches zero as $K_{\mathrm{H}} \to 0$ so that $\Delta \to 0$. The Hiemenz boundary-layer thickness, written now in terms of K, is given by

$$(\Delta)^{-\frac{1}{2}}(\nu/K)^{\frac{1}{2}} \tag{3.13}$$

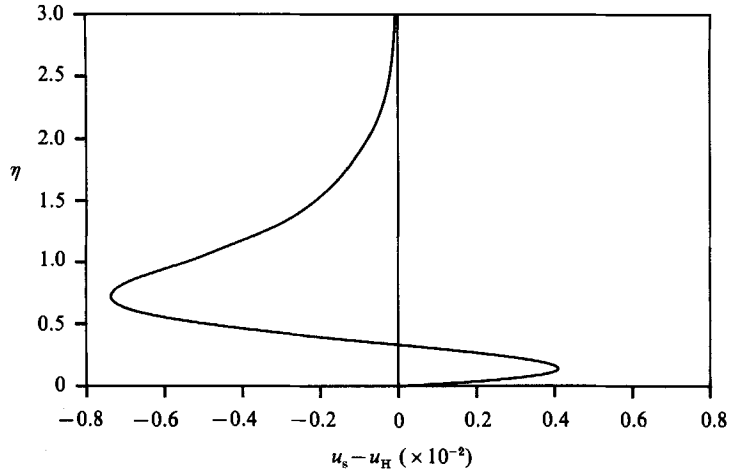

FIGURE 1. Steady-streaming horizontal-velocity component along the wall (at $x = 1$) versus the normal η-coordinate. Here u_H represents the horizontal velocity contribution from Hiemenz flow and u_s the total steady horizontal velocity component.

so that when $\Delta = O(1), K \sim K_H$ and (3.13) reduces to the steady Hiemenz boundary-layer thickness. For the Hiemenz and steady-streaming boundary layers to coincide one would expect Δ to be of the order $\hat{\epsilon}^2$. To investigate this case, Δ is rescaled as follows:

$$\Delta = \bar{\Delta}\hat{\epsilon}^2, \quad \bar{\Delta} = O(1). \tag{3.14}$$

If at the end of the analysis we take $\bar{\Delta} = O(\hat{\epsilon}^{-2})$, so that $\Delta = 1$, the previous solution (3.12) should be recovered, with $\delta = 1$, and as $\bar{\Delta} \to 0$ the problem should reduce to that of zero-mean flow.

Equation (2.10) is rescaled on the Stokes-layer thickness ($\hat{\xi} = \hat{\eta}/\hat{\epsilon}, \hat{\psi}(\hat{\xi}, \tau) = \hat{F}(\hat{\eta}/\tau)$) and $\hat{\psi}$ is scaled such that $\bar{\psi} = \hat{\psi}\hat{\epsilon}$, to obtain

$$-\bar{\psi}_{\hat{\xi}\tau} + \bar{\psi}_{\hat{\xi}\hat{\xi}\hat{\xi}\hat{\xi}} + \hat{\epsilon}^2[-\bar{\psi}^2 + \bar{\psi}\bar{\psi}_{\hat{\xi}\hat{\xi}}] = \sin\tau - \hat{\epsilon}^2[\tfrac{1}{2} + \tfrac{1}{2}\cos 2\tau] - \hat{\epsilon}^4[2\bar{\Delta}\cos\tau] - (\bar{\Delta})^2\hat{\epsilon}^6, \tag{3.15a}$$

$$\bar{\psi} = \bar{\psi}_{\hat{\xi}} = 0 \quad \text{at} \quad \hat{\xi} = 0, \tag{3.15b}$$

$$\bar{\psi}_{\hat{\xi}} = \bar{\Delta}\hat{\epsilon}^2 + \cos\tau \quad \text{as} \quad \hat{\xi} \to \infty. \tag{3.15c}$$

The above equation is singular with non-uniformity at infinity. To obtain the outer form of the problem, $\bar{\psi}$ and $\hat{\xi}$ are rescaled such that

$$\bar{G}(\hat{\xi}, \tau) = \bar{\psi}(\hat{\xi}, \tau) - [\hat{\xi}\cos\tau - \cos(\tau - \tfrac{1}{4}\pi)], \tag{3.16a}$$

$$\zeta = \hat{\epsilon}^2\hat{\xi}, \tag{3.16b}$$

and

$$G(\zeta, \tau) = \bar{G}(\hat{\xi}, \tau). \tag{3.16c}$$

This gives for the outer problem

$$-G_{\zeta\tau} + \hat{\epsilon}^2[\zeta G_{\zeta\zeta} - 2G_\zeta]\cos\tau + \hat{\epsilon}^4[G_{\zeta\zeta\zeta\zeta} + G_\tau^2 + GG_{\zeta\zeta} - \cos(\tau - \tfrac{1}{4}\pi)\, G_{\zeta\zeta}] = 2\bar{\Delta}\hat{\epsilon}^2\cos\tau - (\bar{\Delta})^2\hat{\epsilon}^4, \tag{3.17a}$$

$$G_\tau = \Delta \quad \text{as} \quad \zeta \to \infty. \tag{3.17b}$$

Proceeding as before, the solutions to the inner, (3.15), and outer, (3.17), equations are considered to be of the forms

$$\bar{\psi}(\hat{\xi},\tau) = \bar{\psi}_0(\hat{\xi},\tau)+\hat{\epsilon}\bar{\psi}_1(\hat{\xi},\tau)+\tfrac{1}{2}\hat{\epsilon}^2\bar{\psi}_2(\hat{\xi},\tau)+\tfrac{1}{6}\hat{\epsilon}^3\bar{\psi}_3(\hat{\xi},\tau)+\ldots \tag{3.18a}$$

and

$$G(\zeta,\tau) = G_0(\zeta,\tau)+\hat{\epsilon}G_1(\zeta,\tau)+\tfrac{1}{2}\hat{\epsilon}^2G_2(\zeta,\tau)+\tfrac{1}{6}\hat{\epsilon}^3G_3(\zeta,\tau)+\ldots, \tag{3.18b}$$

respectively; again arbitrary functions that appear in the solutions at each order are determined from secularity and matching conditions.

We summarize the results as follows:
In the outer region,

$$G_0(\zeta,\tau) = \hat{f}_0(\zeta), \quad G_1(\zeta,\tau) = \hat{f}_1(\zeta), \tag{3.19a, b}$$

$$G_2(\zeta,\tau) = 4\bar{A}\zeta\sin\tau+2[\zeta\hat{f}_0'-3\hat{f}_0]\sin\tau+\hat{f}_2(\zeta)-\frac{1}{\sqrt{2}}\cos(2\tau+\tfrac{1}{4}\pi), \tag{3.19c}$$

and

$$G_3(\zeta,\tau) = 6[\zeta\hat{f}_1'-3\hat{f}_1]\cos\tau+\hat{f}_3(\zeta). \tag{3.19d}$$

In the inner region

$$\bar{\psi}_0(\hat{\xi},\tau) = [\hat{\xi}\cos\tau-\cos(\tau-\tfrac{1}{4}\pi)]+\mathrm{e}^{-\hat{\xi}/\sqrt{2}}\cos(\tau-\hat{\xi}/\sqrt{2}-\tfrac{1}{4}\pi), \tag{3.20a}$$

$$\bar{\psi}_1(\hat{\xi},\tau) \equiv 0, \tag{3.20b}$$

$$\begin{aligned}\bar{\psi}_2(\hat{\xi},\tau) = \frac{1}{2}\Big[&\frac{13}{\sqrt{2}}-3\hat{\xi}-3\sqrt{2}\,\mathrm{e}^{-\hat{\xi}/\sqrt{2}}\cos(\hat{\xi}/\sqrt{2})-\sqrt{2}\,\mathrm{e}^{-\hat{\xi}/\sqrt{2}}\sin(\hat{\xi}/\sqrt{2})\\&-\frac{1}{\sqrt{2}}\mathrm{e}^{-\sqrt{2}\hat{\xi}}-2\hat{\xi}\,\mathrm{e}^{-\hat{\xi}/\sqrt{2}}\sin(\hat{\xi}/\sqrt{2})-6\,\mathrm{e}^{-\hat{\xi}/\sqrt{2}}\cos(\hat{\xi}/\sqrt{2}-\tfrac{1}{4}\pi)\Big]\\&-\tfrac{1}{2}[\sqrt{2}\cos(2\tau+\tfrac{1}{4}\pi)-\sqrt{2}\,\mathrm{e}^{-\hat{\xi}}\cos(\hat{\xi}-2\tau-\tfrac{1}{4}\pi)-2\hat{\xi}\,\mathrm{e}^{-\hat{\xi}/\sqrt{2}}\sin(\hat{\xi}/\sqrt{2}-2\tau)]\end{aligned} \tag{3.20c}$$

and

$$\bar{\psi}_3(\hat{\xi},\tau) \equiv 0. \tag{3.20d}$$

The functions $\hat{f}_0(\zeta)$, $\hat{f}_1(\zeta)$ and $\hat{f}_2(\zeta)$ satisfy the following relationships:

$$\hat{f}_0'''-\hat{f}_0'^2+\hat{f}_0\hat{f}_0''+(\bar{A})^2 = 0, \tag{3.21a}$$

$$\hat{f}_0(0) = 0, \quad \hat{f}_0'(0) = -\tfrac{3}{4}, \quad \hat{f}_0'(\infty) = \bar{A}; \tag{3.21b}$$

$$\hat{f}_1'''-2\hat{f}_0'\hat{f}_1'+\hat{f}_1\hat{f}_0''+\hat{f}_0\hat{f}_1'' = 0, \tag{3.21c}$$

$$\hat{f}_1(0) = \hat{f}_1'(0) = \hat{f}_1'(\infty) = 0; \tag{3.21d}$$

and

$$\hat{f}_2'''-2\hat{f}_0'\hat{f}_2'+\hat{f}_2\hat{f}_0''+\hat{f}_0\hat{f}_2'' = 0, \tag{3.21e}$$

$$\hat{f}_2(0) = \frac{13}{2\sqrt{2}}, \quad \hat{f}_2'(0) = 0, \quad \hat{f}_2'(\infty) = 0. \tag{3.21f}$$

The only solution to (3.21 c, d) is $\hat{f}_1(\zeta) \equiv 0$ so that once $\hat{f}_0(\zeta)$ is obtained, (3.21 e, f) can be numerically integrated to give $\hat{f}_2(\zeta)$. The function $\hat{f}_3(\zeta)$ is not calculated since two higher-correction terms in both the inner and outer expansions are required before

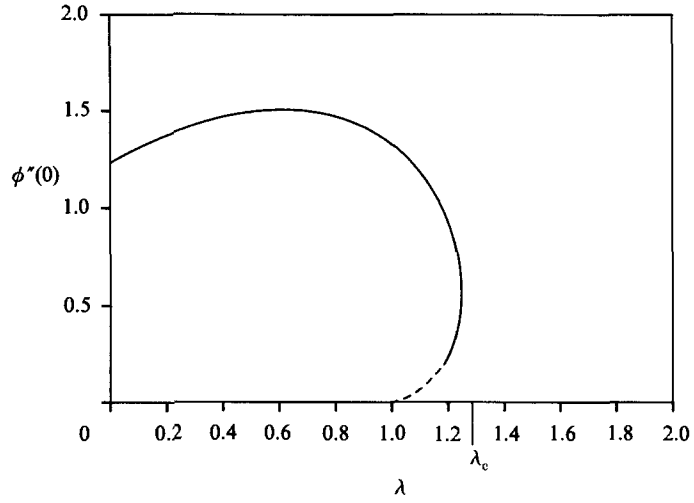

FIGURE 2. Solution branches of system (3.23) with $\lambda = 3/4\bar{A}$ and $\bar{A} = (K_H/K)(\omega/K)$ with $\omega/K \gg 1$. Here $\lambda_c \approx 1.246$. The dashed curve is due to Riley & Weidman (1989).

the governing equation and boundary conditions are known. The composite expansion for $\hat{F}(\hat{\eta}, \tau)$ is then given by

$$\begin{aligned}\hat{F}(\hat{\eta},\tau) = {} & \hat{\eta}\cos\tau + \hat{\epsilon}[\hat{f}_0(\hat{\epsilon}\hat{\eta}) - \cos(\tau - \tfrac{1}{4}\pi) + \mathrm{e}^{-\hat{\eta}/\hat{\epsilon}\sqrt{2}}\cos(\tau - \hat{\eta}/\hat{\epsilon}\sqrt{2} - \tfrac{1}{4}\pi)] \\ & + \tfrac{1}{2}\hat{\epsilon}^2[-\hat{\eta}\,\mathrm{e}^{-\hat{\eta}/\hat{\epsilon}\sqrt{2}}\sin(\hat{\eta}/\hat{\epsilon}\sqrt{2}) + \hat{\eta}\,\mathrm{e}^{-\hat{\eta}/\hat{\epsilon}\sqrt{2}}\sin(\hat{\eta}/\hat{\epsilon}\sqrt{2} - 2\tau)] \\ & + \tfrac{1}{6}\hat{\epsilon}^3\Big[-9\sqrt{2}\,\mathrm{e}^{-\hat{\eta}/\hat{\epsilon}\sqrt{2}}\cos(\hat{\eta}/\hat{\epsilon}\sqrt{2}) - 3\sqrt{2}\,\mathrm{e}^{-\hat{\eta}/\hat{\epsilon}\sqrt{2}}\sin(\hat{\eta}/\hat{\epsilon}\sqrt{2}) \\ & - \frac{3}{2\sqrt{2}}\mathrm{e}^{-\sqrt{2}\hat{\eta}/\hat{\epsilon}} + \frac{3}{\sqrt{2}}\mathrm{e}^{-\hat{\eta}/\hat{\epsilon}}\cos(\hat{\eta}/\hat{\epsilon} - 2\tau - \tfrac{1}{4}\pi) + 12\bar{A}\hat{\epsilon}\hat{\eta}\sin\tau \\ & + 6[\hat{\epsilon}\hat{\eta}\hat{f}_0'(\hat{\epsilon}\hat{\eta}) - 3\hat{f}_0(\hat{\epsilon}\hat{\eta})]\sin\tau - \frac{3}{\sqrt{2}}\cos(2\tau + \tfrac{1}{4}\pi) + 3\hat{f}_2(\hat{\epsilon}\hat{\eta})\Big] + \ldots . \end{aligned} \tag{3.22}$$

System (3.21*a*, *b*) can be rewritten such that $x = (\bar{A})^{\frac{1}{2}}\zeta$ and $\hat{f}_0(\zeta) = (\bar{A})^{\frac{1}{2}}\phi(x)$ to give

$$\phi''' + \phi\phi'' - \phi'^2 + 1 = 0, \tag{3.23a}$$

$$\phi(0) = 0, \quad \phi'(0) = -\lambda, \quad \phi'(\infty) = 1, \tag{3.23b}$$

where $\lambda = 3/4\bar{A}$ and primes denote derivatives with respect to x. This portion of the outer solution represents a stagnation-point flow with an imposed tangential velocity at the surface of the plate opposite in direction to that of the free stream. This situation arises in the present problem owing to the steady streaming (figure 1) generated by the oscillatory flow.

The negative velocity profile of small amplitude that persists outside the Stokes layer is matched within the Hiemenz boundary layer, $(\nu/K_H)^{\frac{1}{2}}$. System (3.23) is interpreted as the matching across this boundary layer of the mean flow with the negative steady streaming profile.

For small λ (large $\bar{A}$), (3.23) can be solved by a perturbation method to yield

$$\phi(x) = F_H(x) - \frac{\lambda}{2c}F_H'(x) + \ldots, \tag{3.24}$$

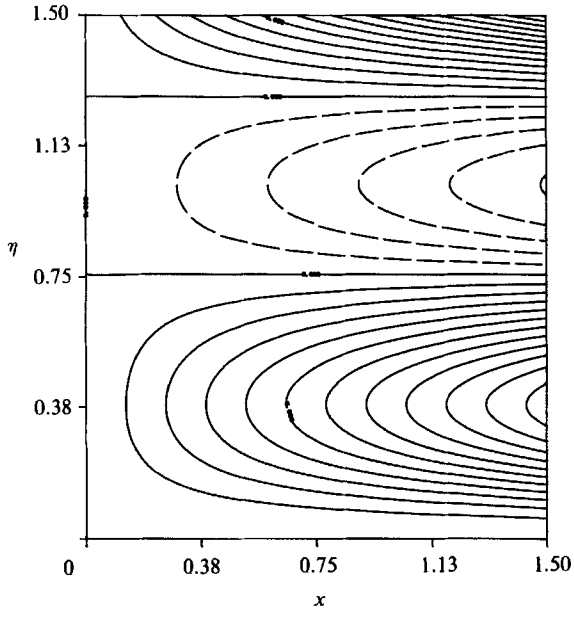

FIGURE 3. Typical streamlines of the steady flow field for $\bar{\Delta} = 2.551$, where $(K_H/K) = \bar{\Delta}(K/\omega)$ and $K/\omega \ll 1$. The line $x = 0$ is the centreline of the flow field.

so that

$$f_0(\hat{\epsilon}\hat{\eta}) \sim (\bar{\Delta})^{\frac{1}{2}} F_H[(\bar{\Delta})^{\frac{1}{2}}\hat{\epsilon}\hat{\eta})] - \frac{3}{8c}(\bar{\Delta})^{\frac{1}{2}} F'_H[(\bar{\Delta})^{\frac{1}{2}}\hat{\epsilon}\hat{\eta})] + \ldots. \tag{3.25}$$

As $\bar{\Delta}$ approaches $\hat{\epsilon}^{-2}$ so that $\Delta \to 1$, (3.22) reduces to (3.12) with $\delta = 1$.

The solution of system (3.23) is sought numerically by using a combination of a Runge–Kutta scheme and a shooting method. The results indicate that there is a critical value of λ, $\lambda_c \approx 1.246$, above which no solutions exist, and for which when $1.19 < \lambda < \lambda_c$ the solution is non-unique (see figure 2). The numerical scheme we use breaks down for values of λ below about 1.19. Recently, Riley & Weidman (1989) have considered a class of Falkner–Skan boundary layers within which system (3.23) is included. By use of careful numerical and asymptotic analysis they too find the value λ_c and are able to continue the curve to values of λ below 1.19. Thus, for system (3.23) there are no solutions for $\lambda > \lambda_c$ and non-uniqueness for $1 < \lambda < \lambda_c$.

The implications of the existence of λ_c in this problem are that there are no solutions for vanishing mean flow and the smallest amount of mean flow allowed is approximately of the order $(3/4\lambda_c)\hat{\epsilon}^2$. As the mean flow vanishes, the Hiemenz-layer scale disappears and this type of similarity is lost. Near the value of λ_c there is no visible difference between the solutions along the two different branches of the curve. Considering only the steady components of the solution (3.22), at λ near λ_c, there exist two cells, a thin one near the surface of the plate and a much thicker one adjusting the direction of the velocities to that of the outer flow (see figure 3). As λ decreases towards zero (following the top branch), the larger cell gets reduced in size until there is an abrupt transition from two cells to no cells. The shrinking of the outer cell can be seen in figure 4 which shows the evolution of the nodes (position of zero velocity) as λ is decreased from λ_c to zero. The maximum horizontal velocities

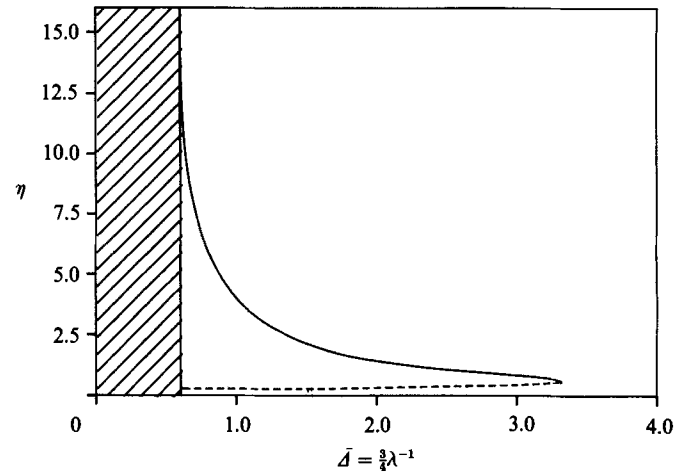

FIGURE 4. The position of the node in the horizontal velocity in the steady flow field as a function of $\bar{A} = (K_H/K)(\omega/K)$: ---, the first node; ——, the second node. Within the shaded region no similarity solutions exist. The lines begin at the position $\bar{A} = 3/4\lambda_c$ and terminate where no reverse flow is present.

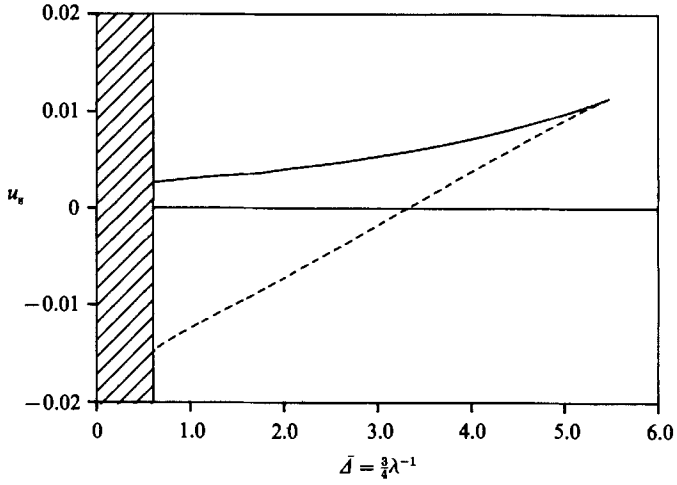

FIGURE 5. The direction and magnitude of the local maximum and minimum horizontal velocity profile (at $x = 1$) for the steady flow field plotted against $\bar{A} = (K_H/K)(\omega/K) = 3/4\lambda$: ——, the first local peak; ---, the second local peak. Within the shaded region no similarity solutions exist. The lines begin at the position $\bar{A} = 3/4\lambda_c$ and terminate where the outer mean flow completely dominates the streaming profile. The cross-over point corresponds to the termination point in figure 4.

present in the cells are shown in figure 5, with the larger cell beginning with a negative velocity which is decreased as the strength of the mean flow increases. The cross-over point, where both velocities become positive, indicates the position of extinction of both cells.

The lengthscales involved in the problem and their various magnitudes are displayed in table 1. Figure 6 contains a summary of the evolution and extinction of cells while showing the various lengthscales.

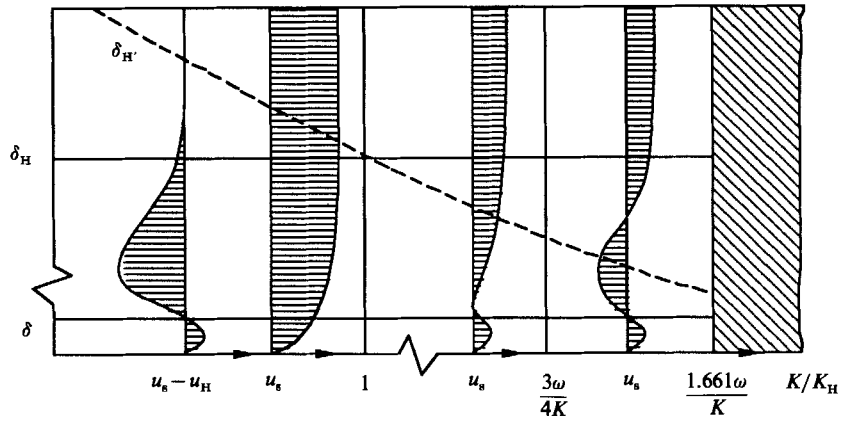

FIGURE 6. The various lengthscales and horizontal velocity profiles (at $x = 1$) versus $(\Delta)^{-1} = K/K_H$ (for K_H fixed). Here u_H represents the horizontal velocity of the Hiemenz flow and u_s the total, steady, horizontal velocity component. For $K/K_H \leqslant 1$ the Stokes-layer thickness $\delta = (\nu/\omega)^{\frac{1}{2}}$ and Hiemenz-layer thickness $\delta_H = (\nu/K_H)^{\frac{1}{2}}$ remain constant while the modulation layer $\delta_{H'} = (\nu/K)^{\frac{1}{2}}$ increases such that $\delta \ll \delta_H \ll \delta_{H'}$. In this region u_s is totally dominated by the mean flow and $u_s - u_H$ is a minor part of u_H. For $K/K_H > 1$, $\delta \ll \delta_{H'} \ll \delta_H$, and there is a noticeable contribution to u_s from $u_s - u_H$. When $\frac{4}{3}(\omega/K) \leqslant K/K_H \leqslant 1.661(\omega/K)$, non-unique profiles exist and for $K/K_H > 1.661(\omega/K)$ the similarity assumption breaks down. The region on the right in which no similarity solutions exist is shaded.

$K \ll K_H$	$K \gg K_H$
Hiemenz (streaming) $\quad \delta_H = (\nu/K_H)^{\frac{1}{2}}$	Hiemenz (streaming) $\quad \delta_H = (\nu/K_H)^{\frac{1}{2}}$
Stokes $\left(\frac{K_H}{\omega}\right)^{\frac{1}{2}}\left(\frac{\nu}{K_H}\right)^{\frac{1}{2}} = \epsilon\delta_H = \left(\frac{\nu}{\omega}\right)^{\frac{1}{2}}$	Stokes $\left(\frac{K}{\omega}\right)^{\frac{1}{2}}\left(\frac{\nu}{K}\right)^{\frac{1}{2}} = \hat{\epsilon}\delta_{H'} = \left(\frac{\nu}{\omega}\right)^{\frac{1}{2}}$
$\delta \ll \delta_H \ll \delta_{H'} = (\nu/K)^{\frac{1}{2}}$	$\delta \ll \delta_{H'} \ll \delta_H$

TABLE 1. Relative lengthscales and magnitudes. δ_H and $\delta_{H'}$ are the magnitudes of the Hiemenz $(\nu/K_H)^{\frac{1}{2}}$ and modulation $(\nu/K)^{\frac{1}{2}}$ boundary layers repectively. δ is the Stokes-layer thickness $(\nu/\omega)^{\frac{1}{2}}$.

4. Discussion

Plane stagnation-point flow is modulated so that the velocity components in the free-stream potential flow are proportional to $K_H + K\cos\omega t$. The flow, including the steady streaming, is examined for K_H and K unit order and high frequency $(\omega/K_H)^{\frac{1}{2}}, (\omega/K)^{\frac{1}{2}} \gg 1$.

If $K_H \geqslant K$, we have the modulated Hiemenz problem in which there are two scales of flow. There is the Stokes-layer thickness $(\nu/\omega)^{\frac{1}{2}}$ and the Hiemenz boundary-layer thickness $(\nu/K_H)^{\frac{1}{2}}$. Figure 6 shows that the steady drift is confined within the Hiemenz layer as shown by Grosch & Salwen (1982) for small modulation amplitude. The flow-induced steady streaming $u_s - u_H$ is outward along the plate and inward above it. When the substantial Hiemenz flow u_H is added to the drift, the total mean flow is only slightly perturbed from steady Hiemenz flow.

If $K \geqslant K_H$, we have a quasi-pulsatile flow; there are again two scales of flow. There is the same Stokes layer and the Hiemenz layer $(\nu/K_H)^{\frac{1}{2}}$. In this case if

$$(K/\omega)(K/K_H) \geqslant 1.661,$$

no similarity solutions exist, while if $\frac{4}{3} \leqslant (K/\omega)(K/K_H) \leqslant 1.661$ the solutions are non-unique (see Riley & Weidman 1989 for details of their numerical results). The drift, when it exists, is always confined to the Hiemenz layer of thickness $(\nu/K_H)^{\frac{1}{2}}$. This drift $u_s - u_H$ is outward along the plate and it returns at a distance away from the plate. The steady Hiemenz flow coupled with the drift results in the appearance of cells close to the plate as can be seen in figure 6.

Finally, the flow considered has strongly non-parallel streamlines and we have shown, following Pedley (1972) and Grosch & Salwen (1982), that for high frequencies, the steady drift can be described without the need to analyse the double boundary layers. When the equivalent of the streamline non-parallelism is small and expansions in its amplitude are used (cf. Rosenblat 1959; Stuart 1966; Riley 1965, 1975), double boundary-layer matching is required.

This work was supported by a grant from the National Aeronautics and Space Administration Program on Microgravity Science and Applications.

REFERENCES

GROSCH, C. E. & SALWEN, H. 1982 Oscillating stagnation point flow. *Proc. R. Soc. Lond.* A **384**, 175–190.

GROTBERG, J. B. 1984 Volume-cycled oscillatory flow in a tapered channel. *J. Fluid Mech.* **141**, 249–264.

HALL, P. 1974 Unsteady viscous flow in a pipe of slowly varying cross-section. *J. Fluid Mech.* **64**, 209–226.

ISHIGAKI, M. 1970 Periodic boundary layer near a two-dimensional stagnation point. *J. Fluid Mech.* **43**, 477–486.

LIGHTHILL, M. J. 1954 The response of laminar skin friction and heat transfer to fluctuations in stream velocity. *Proc. R. Soc. Lond.* A **224**, 1–23.

LONGUET-HIGGINS, M. S. 1953 Mass transport in water waves. *Phil. Trans. R. Soc. Lond.* A **245**, 535–581.

MATUNOBU, Y. 1977 Structure of pulsatile Hiemenz flow and temporal variations of wall shear stress near the stagnation point II. *J. Phys. Soc. Japan* **43**, 326–329.

MORKOVIN, M. V. 1978 Instability, transition to turbulence and predictability. *AGARDograph* no. 236.

PEDLEY, T. J. 1972 Two-dimensional boundary layers in a free stream which oscillates without reversing. *J. Fluid Mech.* **55**, 359–383.

RILEY, N. 1965 Oscillating viscous flows. *Mathematika* **12**, 161–175.

RILEY, N. 1975 Unsteady laminar boundary layers. *SIAM Rev.* **17**, 274–297.

RILEY, N. & WEIDMAN, P. D. 1989 Multiple solutions of the Falkner–Skan equation with a stretching boundary. *SIAM J. Appl. Maths* (to appear).

ROSENBLAT, S. 1959 Torsional oscillations of a plane in a viscous fluid. *J. Fluid Mech.* **6**, 206–220.

ROSENBLAT, S. 1960 Flow between torsionally oscillating disks. *J. Fluid Mech.* **8**, 388–391.

ROSENHEAD, L. 1963 *Laminar Boundary Layers*. Oxford University Press.

SCHLICHTING, H. 1932 Berechnung ebener periodischer Grenzschichtströmungen. *Phys. Z.* **33**, 327–335.

SCHLICHTING, H. 1960 *Boundary Layer Theory*. McGraw-Hill.

SECOMB, T. W. 1978 Flow in a channel with pulsating walls. *J. Fluid Mech.* **8**, 273–288.

STUART, J. T. 1966 Double boundary layers in oscillatory viscous flow. *J. Fluid Mech.* **24**, 673–687.